Effects of hematite on the stabilization of copper, cadmium and phosphorus in a contaminated red soil amended with hydroxyapatite

Hongbiao Cui[a,b], Lulu Shen[a], Xiong Yang[a,b], Shiwen Zhang[a], Qitao Yi[a], Lin Meng[c], Xuebo Zheng[c,**], Qiuya Wang[a], Jun Zhou[b,*]

[a] *School of Earth and Environment, Anhui University of Science and Technology, Huainan, 232001, China*
[b] *Key Laboratory of Soil Environment and Pollution Remediation, Institute of Soil Science, Chinese Academy Sciences, Nanjing, 210008, China*
[c] *Key Laboratory of Tobacco Biology and Processing, Ministry of Agriculture, Tobacco Research Institute of Chinese Academy of Agricultural Sciences, Qingdao, 266101, China*

A B S T R A C T

Iron (Fe) oxides are intimately coupled with phosphorus and closely associated with the bioavailability of potential toxic elements (PTEs) in soil. Thus, Fe oxides may influence the stabilization of PTEs in contaminated soils amended by phosphorus. To evaluate the effects of hematite (HMT) on the stabilization of PTEs, 1–5% (by weight) of HMT was added into a contaminated red soil amended with hydroxyapatite (HAP) to simulate naturally occurring Fe oxides. The stabilization efficiencies of soil copper (Cu) and cadmium (Cd) amended with HAP in soils with low, moderate, and high content of HMT were assessed after a 60-day incubation. HAP treated the soil with high rate HMT decreased the $CaCl_2$-extractable and acid-soluble fractions of Cu and Cd than that of HAP alone. In particular, $CaCl_2$-extractable Cu and Cd in the soil with 5% HMT amended by HAP were 91–95% and 41–68% lower than those amended with only HAP. High content of HMT in soil could decrease the concentration of labile phosphorus in the presence of HAP, but it did not increase the concentration of NaOH-extractable inorganic phosphorus (the fraction bound to Fe oxides). The concentrations of free and crystalline Fe oxides were significantly increased by adding high dosages of HMT with or without HAP. High content of HMT in soil amended by HAP reduced metal phytotoxicity and uptake by wheat shoots than the soil containing HAP without HMT. The results indicate that HMT can promote Cu and Cd stabilization while decrease labile phosphorus in red soil amended with HAP, suggesting that phosphorus-based amendments combined with Fe oxides can be used to stabilize PTEs in contaminated red soils.

1. Introduction

Soil contaminated by potential toxic elements (PTEs) (e.g. cadmium (Cd), copper (Cu), lead, mercury, arsenic, and chromium) have caused public health concerns worldwide (Bandara et al., 2019; He et al., 2019). Large amounts of PTEs are discharged into the soil environment by anthropogenic activities including mining, metal smelting, agrochemical use, and power generation (He et al., 2019). This problem is especially serious in developing countries such as China due to the inadequate enforcement of environmental protection laws in the past (Zhao et al., 2015). PTEs can accumulate in the human body through the food chain and then threaten public health (Bandara et al., 2019; Rinklebe et al., 2019). Therefore, it is urgent to remove or stabilize PTEs in contaminated soils.

It has been reported that the PTEs contents in 21% of agricultural soil samples from five major grain production regions of China exceeded the National Environmental Quality Standard for Soils (GB 15618–1995) (Shang et al., 2018), with the main metal contaminants being Cd, nickel, Cu, zinc, and mercury. The degree of soil contamination was greater in southern China (where red soil is dominant) than northern China. In particular, the standard-exceeding rates of Cd, nickel, and Cu in soils from the southern areas were higher than those in soils from the northern areas (Shang et al., 2018; MEP and MLS, 2014). Currently, there is an urgent need to develop an effective method to deal with PTEs in red soils in southern China.

Chemical stabilization is widely used in farmlands contaminated with PTEs because of its low cost and high efficiency for reducing the migration and bioavailability (Lin et al., 2019; Xu et al., 2017a).

Phosphorus-based materials are considered as promising chemical amendments since they can strongly fix PTEs by forming metal–phosphate precipitates (Mignardi et al., 2012). Hydroxyapatite (HAP) has been extensively applied to stabilize PTEs in soils, sediments, surface water, and ground water (Kazeminezhad et al., 2017; Mignardi et al., 2012). HAP can also increase the content of soil phosphorus in farmlands with low phosphorus release kinetics, making HAP suitable for application in red soils with low pH and low phosphorus availability (Ao et al., 2014; Wang et al., 2015). Thus, HAP shows good potential for stabilizing PTEs in red soils.

After addition of phosphorus-based materials to soil, they react with PTEs such as Cu, Cd, and lead along with other metals (e.g. iron, calcium, and aluminum) (Neidhardt et al., 2018; Wu et al., 2018). Red soils are rich in Fe oxides including hematite (HMT), goethite, magnetite, and ferrihydrite. In most cases, red soils in southern China contain 2%–17% free Fe oxides (Yu et al., 2016). Fe oxides can strongly adsorb PTEs and decrease their bioavailability in soil (Liu et al., 2014; Wang et al., 2019). In addition, Fe oxides have a large adsorption capacity for phosphorus and thus influence its transport, transformation, bioavailability, and geochemical cycling (Fink et al., 2016; Frossard et al., 1995). Therefore, abundant Fe oxides in red soils are expected to compete with metal ions for phosphate released from HAP, thereby decreasing the metal stabilization efficiency of HAP. However, it remains unclear if the interactions between HAP-derived phosphorus and HMT could alter metal stabilization relative to systems containing HAP in the absence of HMT. Answering this question will support the application of phosphorus-based amendments in the stabilization of PTEs for contaminated red soils with various HMT contents.

The aim of this study was to assess the effects of naturally occurring HMT on the stabilization of Cu and Cd in contaminated red soil amended by HAP. The specific objectives were to (i) investigate the changes in soil pH and the contents of $CaCl_2$-extractable Cu and Cd; (ii) determine the chemical transformation of Cu, Cd, phosphorus, and Fe oxides; and (iii) measure the phytotoxicity of Cu and Cd to wheat shoots after a 60-day incubation period in the co-presence of HAP and HMT.

2. Materials and methods

2.1. Experimental materials

Surface paddy soil (0–17 cm) was sampled near a Cu smelter (28°19' N, 117°12' E) in Guixi, Jiangxi Province, southeastern China. After air-drying, the soil was ground and sieved through a 2-mm sieve. Soil total Cu, total Cd, total phosphorus, Olsen phosphorus and pH were 752 mg/kg, 1.04 mg/kg, 445 mg/kg, 51.1 mg/kg and 4.57, respectively. The cation exchange capacity and soil organic carbon were 89.8 mmol/kg and 23.7 g/kg, respectively.

HAP (purity > 96.3%, pH = 7.72) and HMT (α-Fe_2O_3, purity > 99.5%, pH = 9.51) were purchased from Emperor Nano Material Co. Ltd. (Nanjing, China). The XRD patterns of HAP and HMT are shown in the Supplementary Material (Fig. S1).

2.2. Experiment design

A soil incubation experiment was carried out in 1000-mL polyvinyl chloride beakers over a 60-day period. Each beaker contained 500 g of soil manually mixed with HMT and/or HAP. The HAP was added to soil at a 2:1 M ratio of phosphorus to metal (Cu or Cd) (Cao et al., 2009). Previous studies showed the contents of Fe oxides in red soil ranged from 2% to 17% (Yu et al., 2016), and they may influence the bioavailability of PTEs (Almaroai et al., 2014; Wang et al., 2019; Yin et al., 2016). Therefore, 1% (low rate), 3% (moderate rate), and 5% (high rate) HMT (by weight) was added to the contaminated soil to simulate naturally occurring red soil with different contents of Fe oxides. The experiment included eight treatments: untreated soil (CK), 1% HMT (5 g) plus soil (H1), 3% HMT (15 g) plus soil (H3), 5% HMT (25 g) plus

soil (H5), 0.5% HAP (2.5 g) plus soil (HAP), 0.5% HAP (2.5 g) plus 1% HMT (5 g) and soil (HH1), 0.5% HAP (2.5 g) plus 3% HMT (15 g) and soil (HH3), 0.5% HAP (2.5 g) plus 5% HMT (25 g) and soil (HH5). All treatments were conducted in triplicate and incubated at 20–25 °C.

During the 60-day incubation, soil moisture was maintained at 60% of water-holding capacity (WHC) in all beakers by regularly adding deionized water. Soil samples (30 g) were collected at 7, 30, and 60 days for measurements of soil pH and $CaCl_2$-extractable metal contents. The chemical fractions of Cu, Cd, phosphorus, and Fe oxides were analyzed using soil samples collected at 60 days.

2.3. Soil chemical analysis

The main physicochemical characteristics (pH, cation exchange capacity, soil organic carbon, total Cu, Cd, and phosphorus) of the soil were measured based on the method of Cui et al. (2017). Readily available Cu and Cd contents were analyzed after extracting soil (5 g) with 0.01 mol/L $CaCl_2$ solution (25 mL). For quality assurance, all tests were performed in triplicate, and blanks along with certified soil (GBW07408, National Research Center for Certified Reference Materaials, China) and plant (GBW10010, National Research Center for Certified Reference Materials, China) reference materials were analyzed, and the accuracy ranging from 93% to 107%.

2.4. Chemical fractionation analysis

The chemical fractions of Cu and Cd in soil, including acid-soluble (exchangeable and carbonate-bound), reducible (Fe–Mn oxide-bound), oxidizable (organic-bound), and residual metals, were determined using the European Community Bureau of Reference (BCR) sequential extraction procedure (Memoli et al., 2018a). The chemical fractions of soil phosphorus, including: (1) P_{DW}, extracted with deionized water; (2) Pi_{NaHCO3} and Po_{NaHCO3}, extracted with $NaHCO_3$; (3) Pi_{NaOH} and Po_{NaOH}, extracted with NaOH; (4) P_{HCl}, extracted with HCl; and (5) P_{res}, residual P, were analyzed according to Tiessen and Moir (1993). The detailed sequential extraction procedures were given in the Supplementary Material (Text S1 and S2). Free Fe oxides (Fe_f), amorphous Fe oxides (Fe_a) and crystalline Fe oxides (Fe_c) in soil were analyzed using the method described by Jaworska et al. (2016).

2.5. Phytotoxicological assays, antioxidant enzyme activity, and metal uptake analyses

The phytotoxicity tests were performed based on the method of Memoli et al. (2018b). The detailed determination procedures were described in Text S3. The wheat root length and inhibition rate were estimated according to the method of Memoli et al. (2018b).

The superoxide dismutase (SOD) activity in fresh shoots of wheat seedlings was assayed using nitroblue tetrazolium chloride (Beauchamp and Fridovich, 1971). The peroxidase (POD) and catalase (CAT) activities were measured through spectrophotometrical method by monitoring the oxidation of guaiacol by H_2O_2 (Zhang et al., 2007) and the hydrolysis of H_2O_2 (Qiu et al., 2008), respectively. The detailed analytical procedures are provided in the Supplementary Material (Text S4). Moreover, the shoots of wheat seedlings were digested with nitric acid and perchloric acid. The concentrations of Cu and Cd in the extracts were measured using an A3 atomic absorption spectrophotometer (Persee General Instrument, Beijing, China) equipped with a graphite furnace.

2.6. Statistical analysis

Statistical analyses were conducted using SPSS 19.0 (IBM SPSS, Somers, USA). Experimental data were presented as mean values ± standard deviation ($n = 3$). Means among different treatments were subjected to one-way analysis of variance followed by Duncan's test
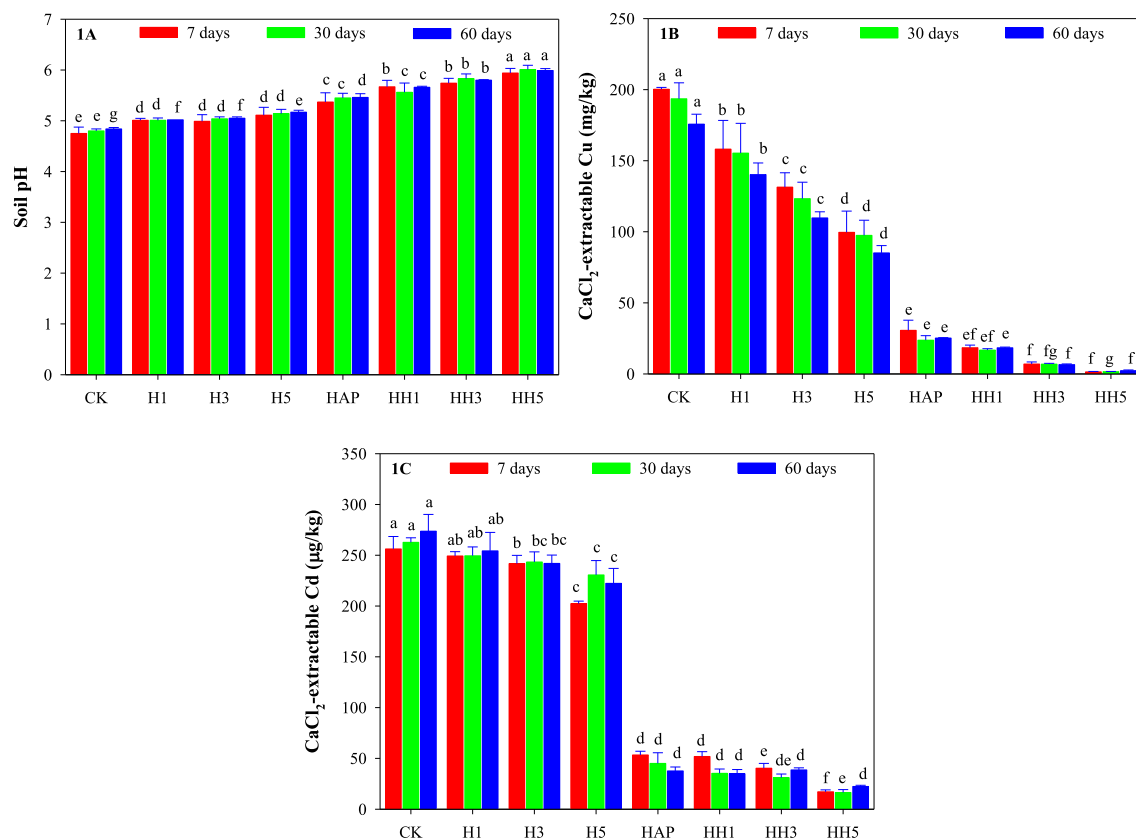
Fig. 1. Changes in pH (A) and the contents of CaCl$_2$-extractable Cu (B) and Cd (C) in contaminated red soil amended with HAP with or without HMT over a 60-day incubation period. Different letters indicate significant differences among treatments. Statistical results of soil pH, CaCl$_2$-extractable Cu and Cd are showed in Table S1. (For interpretation of the references to colour in this figure legend, the reader is referred to the Web version of this article.)
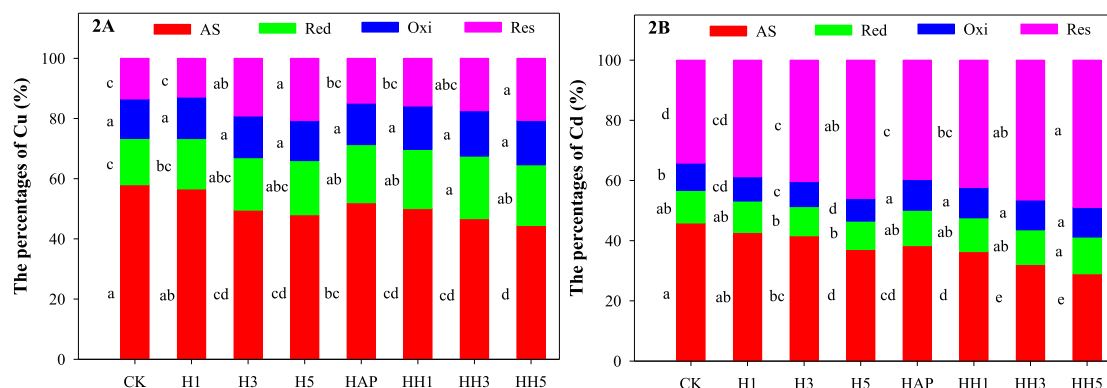

Fig. 2. Chemical fractions of Cu (A) and Cd (B) in contaminated red soil amended with HAP with or without HMT based on BCR sequential extraction. Different letters indicate significant differences among treatments. Statistical results of chemical fractions of Cu and Cd are showed in Table S1. (For interpretation of the references to colour in this figure legend, the reader is referred to the Web version of this article.)

($P < 0.05$). Pearson's correlation coefficients were used to assess the relationships between different variables.

3. Results

3.1. Changes in soil pH and CaCl$_2$-extactable metal contents

All soil samples were acidic with pH values ranging from 4.75 to 6.01 (Fig. 1A). The pH of the control soil was the lowest (4.75–4.84) among all treatments. As the dosage of HMT increased from 1% to 5%

in the absence of HAP, the soil pH changed from 5.01 to 5.02 to 5.11–5.17. The pH values of the soils treated with only HAP were 0.62–0.65 units higher than the pH of the control soil. The highest soil pH was found in treatment HH5, for which the pH was 0.53–0.57 times higher than those of the soils treated with only HAP. For all treatments, soil pH did not change significantly over the 60 days of incubation.

As expected, the highest contents of CaCl$_2$-extractable Cu (176–200 mg/kg) and Cd (256–274 μg/kg) were found in the control soil (Fig. 1B and C). CaCl$_2$-extractable Cu and Cd were decreased with the increasing HMT dosage, and they were 50–52% and 12–21% lower

in HH than the control soil, respectively. Moreover, treatment with HAP alone also decreased $CaCl_2$-extractable metal content compared to the control, and the metal content decreasing in the following order: CK > H1 > H3 > H5 > HAP > HH1 > HH3 > HH5. As the dosage of HMT increased in the absence of HAP, the $CaCl_2$-extractable Cu and Cd content decreased significantly except for $CaCl_2$-extractable Cd at 60th day. For example, the $CaCl_2$-extractable Cu and Cd contents in treatment HH5 were 93% and 63% lower, than those of the samples treated with HAP alone at 30th day, respectively.

3.2. Transformation of soil Cu and Cd fractions

The sequential extraction results (Fig. 2A) shows that Cu (58%) and Cd (46%) in the control soil primarily occurred in the acid-soluble fraction. Compared to the control soil, soil with high content of HMT decreased the acid-soluble fractions of both metals in a dosage-dependent manner. For example, acid-soluble fractions of Cu and Cd in HH were 17% and 19% lower than the control soil, respectively. Treatment with HAP in soil with or without HMT also decreased the acid-soluble fractions compared to the control; the acid-soluble fractions of Cu and Cd in treatment HH5 (15% and 24%, respectively) were lower than in the sample treated with HAP alone.

Compared to the control, soil with 1–5% HMT did not change the reducible fractions of Cu and Cd. However, treatment with HAP in soil with or without HMT increased the reducible fraction of Cu but not Cd compared to the control. No significant differences were observed in the oxidizable fraction of Cu among the treatments. In contrast, treatment with HAP in soil with or without HMT increased the oxidizable fraction of Cd compared to the control. Moreover, the residual fractions of Cu and Cd were both increased in soil with high dosage of HMT, which were 53% and 42% higher in H5 than the control soil, respectively. Similarly, the residual fractions of Cu and Cd were respectively 38% and 23% higher in treatment HH5 compared to the sample treated with only HAP.

3.3. Transformation of soil phosphorus and Fe oxide fractions

Generally, soil with high content of HMT did not significantly change the distribution of soil phosphorus fractions compared to the control (Table 1). However, treatment with HAP in soil with or without HMT increased the fractions of P_{DW}, $P_{iNaHCO3}$, P_{iNaOH}, P_{HCl}, and P_{res}, whereas it decreased the fraction of P_{oNaOH} relative to the control. For example, the fractions of P_{DW}, $P_{iNaHCO3}$, P_{iNaOH}, P_{HCl}, and P_{res} in treatment with HAP alone were 2.95-, 0.97-, 0.98-, 7.66-, and 1.00-fold higher than those of the control, respectively. However, no significant differences in phosphorus fractions were observed among treatments HAP, HH1, HH3, and HH5, with the following exceptions: treatment HH5 resulted in 11% and 51% reductions in the fractions of $P_{iNaHCO3}$ and $P_{oNaHCO3}$, respectively, and a 21% increase in the P_{oNaOH} fraction relative to treatment with only HAP.

High content of HMT in soil did not decrease labile phosphorus compared to the control. However, treatment with HAP alone increased labile phosphorus compared to the control, while HAP treated soil with 5% HMT significantly decreased labile phosphorus compared to the HAP treatment (Table 1). For example, the fractions of labile and stable phosphorus in treatment HH5 were 18% lower and 6.8% higher, respectively, compared to those in the sample treated with HAP alone. The increase of total phosphorus in treatment of HAP alone was 935 mg/kg compared to the control, but only 18% of it was transformed into the labile fraction, and 74% was transformed into the stable fraction.

The contents of Fe_f (3.69–3.76 mg/kg) and Fe_c (1.99–2.02 mg/kg) in the control soil and the samples treated with HAP were the lowest across all treatments (Fig. 3). The Fe_f and Fe_c contents in soil with 1–5% HMT increased significantly by 1.73–6.69-and 3.18–12.3-fold compared to the control, respectively. HAP treated soils with 1–5% HMT

Table 1
Chemical fractions of phosphorus (mg/kg) in contaminated red soil amended with HAP with or without HMT.

Treatments	P_{DW}	$P_{iNaHCO3}$	$P_{oNaHCO3}$	Labile P	P_{iNaOH}	P_{oNaOH}	Moderately labile P	P_{HCl}	P_{res}	Stable P
CK	16.5 ± 1.81b	92.9 ± 6.21c	31.3 ± 3.32bc	141 ± 9.6d	106 ± 8b	72.0 ± 6.12b	178 ± 13.1b	71.5 ± 8.27b	143 ± 23c	214 ± 21.6d
H1	14.8 ± 1.10b	86.2 ± 8.37c	35.5 ± 1.72b	137 ± 7.7d	107 ± 10b	76.2 ± 8.48ab	183 ± 18.6b	76.5 ± 6.11b	154 ± 14c	231 ± 8.3d
H3	14.4 ± 1.25b	81.3 ± 7.69c	33.3 ± 3.57bc	129 ± 8.0d	106 ± 13b	84.4 ± 4.06a	190 ± 14.1b	82.1 ± 8.86b	145 ± 20c	227 ± 13.2d
H5	14.1 ± 1.63b	75.6 ± 6.04c	38.2 ± 3.08b	128 ± 7.9d	104 ± 12b	78.4 ± 5.68ab	182 ± 13.1b	89.6 ± 16.6b	148 ± 14c	238 ± 22.1d
HA	65.2 ± 4.49a	183 ± 12a	56.1 ± 7.1a	304 ± 18.9a	209 ± 19a	50.0 ± 2.38d	259 ± 17.1a	619 ± 35a	285 ± 19ab	905 ± 16.3bc
HH1	64.4 ± 5.32a	186 ± 10a	33.3 ± 2.77bc	284 ± 6.1ab	213 ± 11a	45.2 ± 3.37d	258 ± 14.5a	616 ± 67a	266 ± 35b	882 ± 46.6c
HH3	63.4 ± 5.50a	171 ± 11ab	32.5 ± 4.74bc	267 ± 20.0bc	206 ± 24a	41.1 ± 4.41d	247 ± 27.0a	636 ± 35a	305 ± 37ab	941 ± 38.3ab
HH5	59.4 ± 5.68a	164 ± 16b	27.7 ± 2.63c	251 ± 12.6c	190 ± 16a	60.3 ± 5.00c	250 ± 16.2a	649 ± 46a	317 ± 20a	966 ± 26.0a

Note: Mean (n = 3) and standard deviation followed by different letters are significantly different ($P < 0.05$). P_{DW}, deionized water soluble phosphorus; $P_{iNaHCO3}$, NaHCO$_3$-extractable inorganic phosphorus; $P_{oNaHCO3}$, NaHCO$_3$-extractable organic phosphorus; Labile phosphorus, including P_{DW}, $P_{iNaHCO3}$ and $P_{oNaHCO3}$; P_{iNaOH}, NaOH-extractable inorganic phosphorus; P_{oNaOH}, NaOH-extractable organic phosphorus; Moderately labile phosphorus, including P_{iNaOH} and P_{oNaOH}; P_{HCl}, HCl-extractable phosphorus; Stable P, residual phosphorus; P_{res}, residual phosphorus; Stable P, including P_{HCl} and P_{res}.
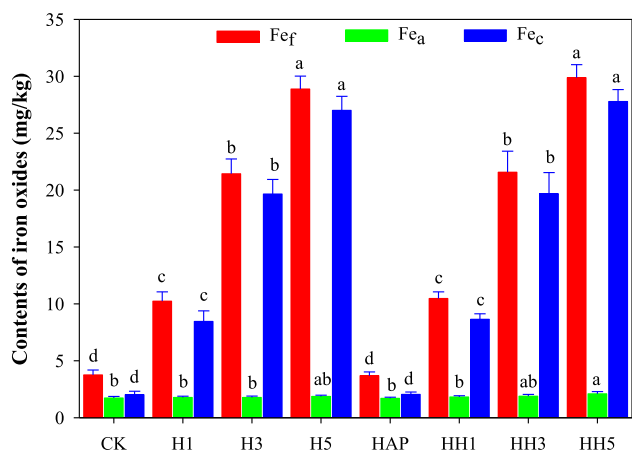
Fig. 3. Fractions of Fe oxides in contaminated red soil with amended with HAP with or without HMT. Fe_f, free Fe oxides; Fe_a, amorphous Fe oxides; and Fe_c, crystalline Fe oxides. Means ($n = 3$) and standard deviations with different letters above the column indicate significant differences at $P < 0.05$. Statistical results of Fe oxides fractions are showed in Table S2. (For interpretation of the references to colour in this figure legend, the reader is referred to the Web version of this article.)

also increased the Fe_f and Fe_c contents compared to the HAP alone, and the extent of the increase depended on the HMT dosage. No significant differences in Fe_a content were found among HAP treated soils with or without HMT.

3.4. Growth inhibition, antioxidant enzyme activities, and metal uptake in wheat

The inhibition rates of wheat roots in H5, HH3, and HH5 were 4.9%,

10%, and 6.0% lower than the control, respectively (Fig. 4A). Soil with 1–5% HMT and/or HAP all decreased CAT, POD, and SOD activities in wheat shoots compared to the control (Fig. 4A and B), and the extent of decrease depended on the HMT dosage. For example, CAT activity decreased from 221 to 132 U/g FW (fresh weight) as the HMT dosage ranged from 1% to 5% in the presence of HAP.

The highest contents of Cu (119 mg/kg) and Cd (384 µg/kg) in wheat shoots were found in the control (Fig. 4C). High content of HMT in soil promoted the reduction of Cu and Cd in wheat shoots, for example, the Cu contents in wheat shoots in treatments H1 and H5 were 23% and 42% lower compared to the control, respectively. Meanwhile, the Cu and Cd contents in treatment HAP alone were 52% and 49% lower than in treatment H5, respectively. No significant differences in the Cu and Cd contents in wheat shoots were observed among treatments HH1, HH3, and HH5.

4. Discussion

4.1. Effect of bioavailable of Cu and Cd

The high efficiencies of HAP on the stabilization of Cu and Cd were well demonstrated in this study. HAP increased soil pH and decreased bioavailable Cu and Cd, in agreement with findings of Mignardi et al. (2012) and Wei et al. (2016). The increase of soil pH with the application of HAP may be due to the dissolution of HAP neutralized protons (H^+) (Sun et al., 2018). The stabilization of Cu and Cd by HAP were possibly via ion exchange, coprecipitation, surface complexation, and precipitation (Fig. 5) (Kazeminezhad et al., 2017; Sun et al., 2018).

Moreover, high dosage of HMT in soil also promoted the reduction of bioavailable Cu and Cd, but the decrease extent was less than that of HAP alone. It may be due to the maximum adsorption capacities of Cu and Cd are 200 and 43.5 mg/g for HAP, and 143 and 14.7 mg/g for HMT, respectively (our unpublished data). Thus, HAP alone was more
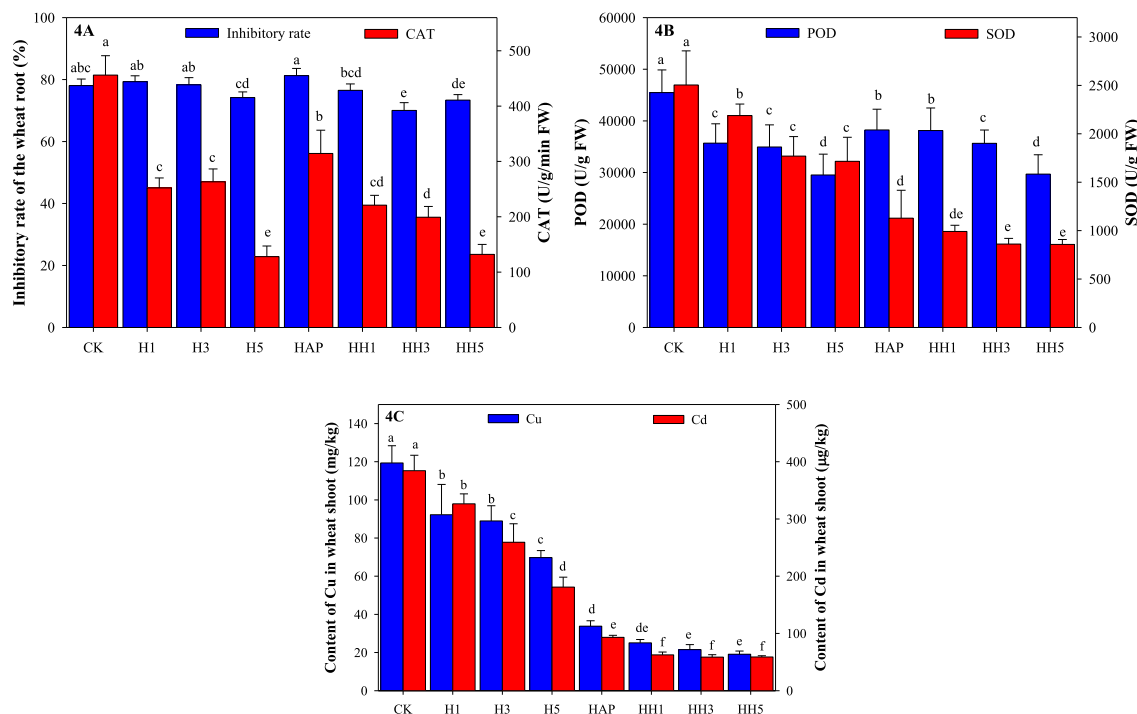

Fig. 4. Inhibition rates of wheat roots and catalase (CAT) activity (A), peroxidase (POD) and superoxide dismutase (SOD) activities (B), and metal uptake in wheat shoots (C) in contaminated red soil amended with HMT and/or HAP. Means ($n = 3$) and standard deviations followed by different letters are significantly different at $P < 0.05$. Statistical results of inhibition rates, CAT, POD,ptake in wheat shoots are showed in Table S2. (For interpretation of the references to colour in this figure legend, the reader is referred to the Web version of this article.)
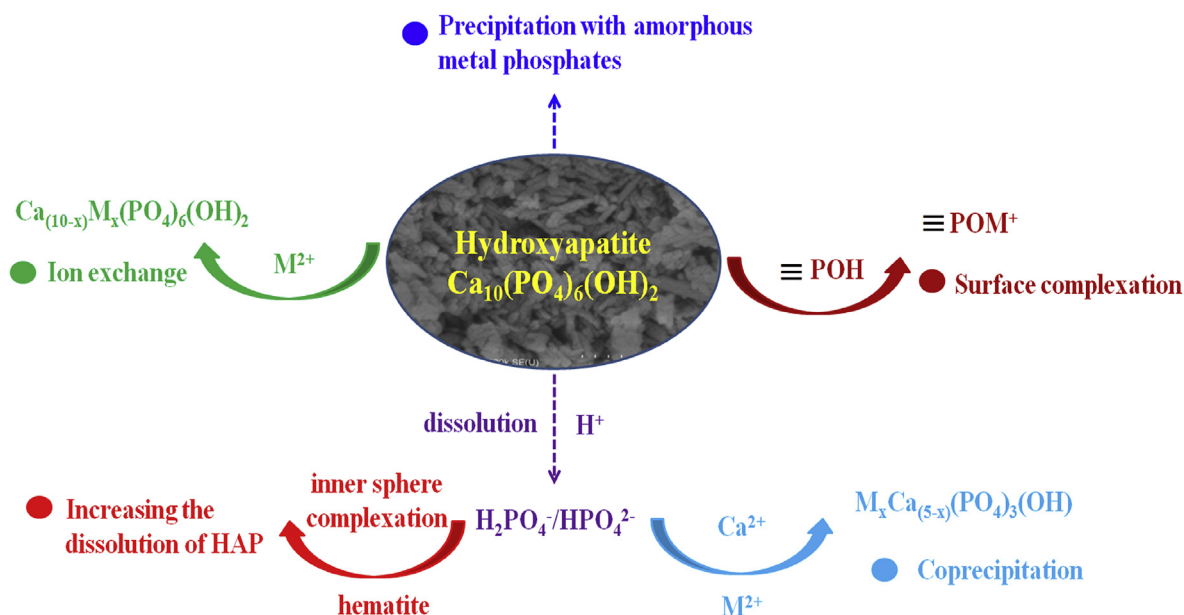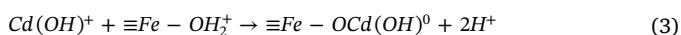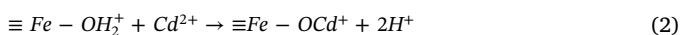
Fig. 5. Adsorption mechanism of PTEs by hydroxyapatite (HAP) in contaminated red soil. M indicates metal ions. (For interpretation of the references to colour in this figure legend, the reader is referred to the Web version of this article.)

effective at decreasing the bioavailability of Cu and Cd compared to HMT. The mechanisms of HMT on the stabilization of Cu and Cd may be due to the generation of Fe–OH groups on its surface (Eq. (1)) during incubation and then adsorb metals through inner-sphere complexation (Eqs. (2) and (3)) (Lee et al., 2012; Li et al., 2019; Zhang et al., 2014, 2016). Similar to HAP, high content of HMT in soil slightly increased soil pH and the increase extent depended on the dosage of HMT. It may result from the high pH of HMT itself (i.e., 9.51 at a 1:2.5 HMT-to-water ratio) and the acidic pH (4.57) of red soil, which could promote the dissolution of HMT. Furthermore, Fe-reductive dissolution could consume H^+ and thus increase soil pH (Oppong-Anane et al., 2018; Yu et al., 2016), in agreement with findings of Friesl et al. (2006) and Li et al. (2012). Although the reductive dissolution of Fe oxides can reduce the number of sorption sites and result in the release of metals on the surfaces of Fe oxides, Fe reduction can increase soil pH and thus increase metal adsorption (Yuan et al., 2019). Therefore, the readily available (CaCl$_2$-extractable) Cu and Cd contents in red soil generally decreased with increasing HMT dosage. However, previous studies indicated that magnetite and HMT reduced soil pH due to the hydrolysis of Fe ions and surface complexation of Fe–OH groups with other metal ions (Yuan et al., 2019; Zhou et al., 2012). This discrepancy might be explained by higher acidity of the soil used in this study compared to the red soils used in previous studies; the higher acidity of the soil used herein might have resulted in a higher Fe oxide dissolution rate.

$$\equiv Fe - OH + H^+ \rightarrow \equiv Fe - OH_2^+ \tag{1}$$

$$\equiv Fe - OH_2^+ + Cd^{2+} \rightarrow \equiv Fe - OCd^+ + 2H^+ \tag{2}$$

$$Cd(OH)^+ + \equiv Fe - OH_2^+ \rightarrow \equiv Fe - OCd(OH)^0 + 2H^+ \tag{3}$$

According to Bogusz and Oleszczuk (2018) and Wen et al. (2016), the acid-soluble fraction of metals has the highest toxicity to biota, the reducible and oxidizable fractions are potentially bioavailable to plants, and the residual fraction is considered stable. The results of the current study indicated that soil with high content of HMT could effectively decrease the bioavailability of Cu and Cd in red soil by transforming the metals from the acid-soluble fraction to the residual fraction. Moreover, the acid-soluble fractions of both Cu ($P = -0.637$) and Cd ($P = -0.836$) had a significant negative correlation with soil pH (Table 2). Likewise, Loganathan et al. (2012) and Yuan et al. (2019) found that increasing soil pH could promote the stabilization of PTEs in

acidic soils because the majority of metals have low solubility in neutral and alkaline conditions. Metals in the reducible fraction are bound to hydrous and amorphous Fe–Mn oxides (Wen et al., 2016). Herein, high dosage of HMT in soil did not substantially increase the reducible fractions of Cu and Cd bound to Fe oxides. This may be because the inner-sphere complexes of the metals are relatively stable (Li et al., 2019), and 0.1 mol/L hydroxylamine hydrochloride could not disrupt the metal–Fe complexation.

In theory, HMT may also compete with metal ions for phosphate and promote the dissolution of HAP, thereby affecting the co-precipitation and formation of metal–phosphate precipitates (Mignardi et al., 2012; Xu et al., 2017b). Calcium ions may also substitute for metals and decrease the inner-sphere complexation of HMT (Eq. (2)) (Li et al., 2019). Thus, the interaction between HAP and HMT thus may reduce their own adsorption capacities for Cu and Cd. Moreover, the net decrease of ΔCaCl$_2$-extractable Cu/Cd$_{HH5-CK}$ was less than the sum of ΔCaCl$_2$-extractable Cu/Cd$_{H5-CK}$ plus ΔCaCl$_2$-extractable Cu/Cd$_{HAP-CK}$. This result also clearly suggests that the stabilization of Cu and Cd by HAP was influenced in the presence of HMT. Nevertheless, the negative effects of HAP–HMT interaction on the stabilization efficiency of metals by HAP were lower than the positive effects induced by HMT adsorption for metals. Therefore, HAP treated soil with high content of HMT were more effective to decrease bioavailable Cu and Cd compared to HAP alone.

4.2. Effects of phosphorus and Fe oxide fractions, and phytotoxicity

Our study showed that phosphorus in the red soil mainly occurs in the residual fraction, suggesting the low activity of phosphorus in red soil. NaOH-extractable phosphorus includes inorganic and organic phosphorus associated with Fe, aluminum, and clay minerals on the soil surface (Hedley et al., 1982; Negassa and Leinweber, 2009). Herein, high content of HMT in soil did not increase P$_{iNaOH}$ in the red soil, suggesting that vivianite was not formed in the soil during incubation. This result may be attributed to inner-sphere ligand exchange, in which phosphate was adsorbed on the HMT surface to form monodentate bi-nuclear and monodentate mononuclear complexes (Wang et al., 2019; Xu et al., 2017b). The phosphorus extracted by HCl is considered to be Ca–P minerals (stable phosphorus) (Negassa and Leinweber, 2009). Thus, HAP treated soils with or without HAP increased HCl–P in the red

Table 2

Correlation coefficients between soil pH, Cu and Cd bioavailability, iron oxide fractions, phosphorus fractions, antioxidant enzyme activities in wheat shoots, and Cu and Cd uptake by wheat shoots (n = 24).

	pH	Ca–Cu	Ca–Cd	AS-Cu	AS-Cd	Fe_f	Fe_a	Fe_c	P_{DW}	P_{iNaHCO_3}	Pi_{NaOH}	P_{HCl}	P_{res}	RI	CAT	POD	SOD	Cu-P	Cd-P
pH	1	-0.947**	-0.937**	-0.637**	-0.836**	0.402	0.500*	0.398	0.877**	0.821**	0.844**	0.917**	0.910**	-0.520**	-0.595**	-0.356	-0.913**	-0.944**	-0.922**
Ca-Cu		1	0.957**	0.666**	0.789**	-0.352	-0.384	-0.349	-0.890**	-0.840**	-0.867**	-0.920**	-0.891**	0.409*	0.600**	0.364	0.951**	0.973**	0.982**
Ca-Cd			1	0.531**	0.747**	-0.119	-0.313	-0.115	-0.972**	-0.946**	-0.950**	-0.984**	-0.946**	0.314	0.390	0.175	0.910**	0.944**	0.933**
AS-Cu				1	0.482*	-0.642**	-0.483*	-0.641**	-0.438*	-0.291	-0.339	-0.445*	-0.532**	0.442*	0.649**	0.552**	0.617**	0.606**	0.670**
AS-Cd					1	-0.470*	-0.414*	-0.468*	-0.669**	-0.624**	-0.640**	-0.724**	-0.736**	0.475*	0.552**	0.336	0.755**	0.785**	0.776**
Fe_f						1.000	0.593**	1.000**	-0.040	-0.137	-0.061	0.053	0.116	-0.640**	-0.814**	-0.704**	-0.345	-0.303	-0.360
Fe_a							1	0.582**	0.226	0.170	0.196	0.303	0.347	-0.431*	-0.581**	-0.495**	-0.448*	-0.426*	-0.369
Fe_c								1	-0.044	-0.141	-0.065	0.048	0.112	-0.639**	-0.812**	-0.702**	-0.341	-0.299	-0.357
P_{DW}									1	0.966**	0.967**	0.982**	0.922**	-0.254	-0.241	-0.022	-0.851**	-0.896**	-0.868**
P_{iNaHCO_3}										1	0.963**	0.982**	0.881**	-0.179	-0.156	0.061	-0.812**	-0.847**	-0.811**
Pi_{NaOH}											1	0.958**	0.856**	-0.225	-0.227	0.036	-0.833**	-0.871**	-0.844**
P_{HCl}												1	0.932**	-0.291	-0.315	-0.090	-0.885**	-0.923**	-0.892**
P_{res}													1	-0.305	-0.339	-0.190	-0.845**	-0.889**	-0.848**
RI														1	0.518**	0.440*	0.440*	0.427*	0.457*
CAT															1	0.791**	0.596**	0.599**	0.614**
POD																1	0.457*	0.402	0.408*
SOD																	1	0.964**	0.956**
Cu-P																		1	0.971**
Cd-P																			1

Ca–Cu, CaCl₂-extractable Cu; Ca–Cd, CaCl₂-extractable Cd; AS-Cu, acid-soluble fraction of Cu; AS-Cd, acid-soluble Cd; Fe_f, free Fe oxides; Fe_a, amorphous Fe oxides; and Fe_c, crystalline Fe oxides.; P_{DW}, deionized water soluble phosphorus; P_{iNaHCO_3}, NaHCO₃-extractable inorganic phosphorus; Pi_{NaOH}, NaOH-extractable inorganic phosphorus; P_{HCl}, HCl-extractable phosphorus; P_{res}, residual phosphorus; RI, inhibition rate of wheat roots; SOD, superoxide dismutase activity; POD, peroxidase activity; CAT, catalase activity; Cu–P, Cu accumulation by wheat shoots; and Cd–P, Cd accumulation by wheat shoots.

**P < 0.01; *P < 0.05.

soil.

Five phosphorus fractions (P_{DW}, $P_{iNaHCO3}$, P_{iNaOH}, P_{HCl}, and P_{res}) were significantly negatively correlated with available Cu and Cd in the red soil (Table 2). This indicates the high potential of phosphorus-containing amendments for the stabilization of PTEs in contaminated red soil. It should be noted that treatment with HAP substantially increased labile phosphorus (P_{DW}, $P_{iNaHCO3}$, and $P_{oNaHCO3}$) compared to the control. Particularly, the high contents of P_{DW} may be leached from the soil, causing eutrophication in the agricultural ecosystem. Moreover, the dosages of HAP (1–5% by weight) used in previous studies (Sun et al., 2018; Wei et al., 2016) were higher than the dosage used in this study (0.5% by weight), potentially leading to a higher risk of eutrophication. Fortunately, the fraction of labile phosphorus in HH5 was 18% lower compared to that in HAP alone. Hence, the dosages of phosphorus-based amendments must be strictly limited, and HAP amended soil with high content of HMT is beneficial to the reduction of eutrophication risk.

The changes in the fractions of Fe oxides controlled by oxidation and reduction conditions have pronounced effects on transformation of PTEs fractions in soil (Yu et al., 2016). Fe oxides in this study were mainly present in the free and crystalline forms, and Fe_f and Fe_c increased in red soil with HMT ranged from 1% to 5% under a WHC of 60%. Moreover, the application of HAP had little effect on the transformation of Fe oxides under the same content of HMT (e.g., treatment H1 vs. HH1). Although Fe oxides are considered to be the most active minerals in soil (Chen et al., 2013), no significant differences in the transformation of Fe oxides were observed in this study. This indicates that short term incubation did not promote the transformation of Fe oxides in HMT-containing red soil in the presence of HAP.

The release of antioxidant enzymes can protect plants from damage by metal contaminants. For example, SOD can convert $O^{.2-}$ to H_2O_2 and O_2, whereas CAT and POD protect cells from oxidant stress by catalyzing H_2O_2 hydrolysis (de Araújo et al., 2017). Similar to the trends in the bioavailability of soil Cu and Cd, HAP treated soils with or without HMT were most effective to decrease SOD, POD, and CAT activities in wheat shoots. This indicates that the phytotoxicity of Cu and Cd was reduced in HAP amended red soil with high content of HMT. In most cases, the antioxidant enzyme activities and metal uptake in wheat shoots were significantly positively correlated with the contents of $CaCl_2$-extractable and acid-soluble fractions of Cu and Cd (Table 2). All the results indicate that the phytotoxicity of Cu and Cd in red soil decreased with decreasing bioavailability of these metals, and high content of HMT promoted the decrease in metal phytotoxicity in the presence of HAP.

In short, the results of this study show that HMT altered the stabilization efficiency of Cu and Cd by HAP, whereas a combination of HMT and HAP was more effective than HAP alone to stabilize PTEs, decrease labile phosphorus, and reduce metal phytotoxicity in red soil. Similarly, Liu and Zhao (2007) used a iron phosphate nanoparticles ($Fe_3(PO_4)_2$) to stabilize Pb and found about 50% reduction of soluble phosphate in $Fe_3(PO_4)_2$ treated soil than that in Na_3PO_4. In addition, Fe oxides and iron powder are very cheap and readily available (Mariussen et al., 2018; Min et al., 2017; Yuan and Liu, 2013). Therefore, Fe oxides in red soil are beneficial to the stabilization of Cu and Cd by phosphorus-based amendments, and we suggest that the combination of phosphate-based amendments and Fe oxides could be used to stabilize PTEs in contaminated red soils. However, this study neglected the fact that the predominant Fe oxides in most red paddy soils are goethite, HMT, lepidocrocite, maghemite, and ferrihydrite (Li et al., 2006). While HMT (crystalline Fe oxide) was used as a representative Fe oxide in this study, its properties are considerably different those of ferrihydrite (amorphous Fe oxide) (Zhu et al., 2019). Therefore, it is necessary to further study the effects of Fe oxides on PTEs stabilization while considering the composition of Fe oxides in natural soil.

5. Conclusions

After 60 days of incubation, HAP amended soils with high content of HMT exhibited lower $CaCl_2$-extractable and acid-soluble fractions of Cu and Cd compared to the control soil under a WHC of 60%. Generally, increasing the dosage of HMT decreased soil Cu and Cd bioavailability in the presence of HAP. HAP amended soils with high content of HMT decreased soil labile phosphorous while decreasing metal phytotoxicity to wheat seedlings. The results suggest that the combination of phosphate-based amendments and Fe oxides could be used to stabilize PTEs in contaminated red soils.

Credit author statement

Jun Zhou, Writing - review & editing, Writing - original draft, Visualization, Investigation, Supervision, Resources, Project administration, Funding acquisition, Methodology, Conceptualization. Xuebo Zheng; Conceptualization, Methodology, Funding acquisition, Project administration, Resources, Supervision, Validation, Investigation, Visualization, Writing - original draft, Writing - review & editing. Hongbiao Cui: Methodology, Investigation, Writing - original draft. Lulu Shen: Formal analysis, Investigation, Visualization. Shiwen Zhang: Resources, Visualization, Writing - review & editing. Qiuya Wang; Investigation, Visualization. Qitao Yi; Visualization, Writing - review & editing. Lin Meng: Visualization, Writing - review & editing. Xiong Yang: Formal analysis, Investigation, Visualization.

Declaration of competing interest

The authors declare no conflict of interest.

Appendix B. Supplementary data

Supplementary data to this article can be found online at https://doi.org/10.1016/j.ecoenv.2020.110830.

References

Almaroai, Y.A., Vithanage, M., Rajapaksha, A.U., Lee, S.S., Dou, X., Lee, Y.H., Sung, J., Ok, Y.S., 2014. Natural and synthesised iron-rich amendments for as and pb immobilisation in agricultural soil. Chem. Ecol. 30 (3), 267–279.

Ao, J., Chen, Z., Wu, M., Lu, X., Huang, Z., Liao, H., 2014. Phosphorus fractions of red soils in Guangdong province of south China and their bioavailability for five crop species. Soil Sci. 179, 514–521.

Bandara, T., Franks, A., Xu, J., Bolan, N., Tang, C., 2019. Chemical and biological immobilization mechanisms of potentially toxic elements in biochar-amended soils. Crit. Rev. Environ. Sci. Technol. (4), 1–77.

Beauchamp, C., Fridovich, I., 1971. Superoxide dismutase: improved assays and an assay applicable to acrylamide gels. Anal. Biochem. 44 (1), 276–287.

Bogusz, A., Oleszczuk, P., 2018. Sequential extraction of nickel and zinc in sewage sludge- or biochar/sewage sludge-amended soil. Sci. Total Environ. 636, 927–935.

Cao, X.D., Wahbi, A., Ma, L., Li, B., Yang, Y.L., 2009. Immobilization of Zn, Cu, and Pb in contaminated soils using phosphate rock and phosphoric acid. J. Hazard Mater. 164 (2–3), 555–564.

Chen, M.J., Cao, F., Li, F.B., Liu, C.S., Tong, H., Wu, W.J., Hu, M., 2013. Anaerobic transformation of DDT related to iron (III) reduction and microbial community structure in paddy soils. J. Agric. Food Chem. 61, 2224–2233.

Cui, H.B., Yang, X., Xu, L., Fan, Y.C., Yi, Q.T., Li, R.Y., Zhou, J., 2017. Effects of goethite on the fractions of Cu, Cd, Pb, P and soil enzyme activity with hydroxyapatite in heavy metal-contaminated soil. RSC Adv. 7, 45869–45877.

de Araújo, R.P., de Almeida, A.A.F., Pereira, L.S., Mangabeira, P.A.O., Souza, J.O.,

Pirovani, C.P., Ahnert, D., Baligar, V.C., 2017. Photosynthetic, antioxidative, molecular and ultrastructural responses of young cacao plants to Cd toxicity in the soil. Ecotoxicol. Environ. Saf. 144, 148–157.

Fink, J.R., Inda, A.V., Tiecher, T., Barrón, V., 2016. Iron oxides and organic matter on soil phosphorus availability. Cienc. E Agrotecnol 40 (4), 369–379.

Friesl, W., Friedl, J., Platzer, K., Horak, O., Gerzabek, M.H., 2006. Remediation of contaminated agricultural soils near a former Pb/Zn smelter in Austria: batch, pot and field experiments. Environ. Pollut. 144 (1), 40–50.

Frossard, E., Brossard, M., Hedley, M.J., Meterell, A., 1995. Reactions controlling the cycling of P in soils. In: Tiessen, H. (Ed.), Phosphorus in the Global Environment. Wiley, New York, pp. 107–137 SCOPE 54, Ch. 7.

He, L., Zhong, H., Liu, G., Dai, Z., Brookes, P.C., Xu, J., 2019. Remediation of heavy metal contaminated soils by biochar: mechanisms, potential risks and applications in China. Environ. Pollut. 252, 846–855.

Hedley, M.J., Stewart, J.W.B., Chauhan, B.S., 1982. Changes in inorganic and organic soil phosphorus fractions induced by cultivation practices and by laboratory incubations. Soil Sci. Soc. Am. J. 46, 970–976.

Jaworska, H., Dąbkowska-Naskręt, H., Kobierski, M., 2016. Iron oxides as weathering indicator and the origin of Luvisols from the Vistula glaciation region in Poland. J. Soils Sediments 16 (2), 396–404.

Kazeminezhad, I., Ahmadizadeh, S., Zargar, B., Babaei, A.A., 2017. Behaviors and mechanisms of copper adsorption using highly efficient nanostructured superparamagnetic hydroxyapatite. Desalin. Water. Treat. 67, 247–260.

Lee, S.M., Laldawngliana, C., Tiwari, D., 2012. Iron oxide nano-particles-immobilized-sand material in the treatment of Cu(II), Cd(II) and Pb(II) contaminated waste waters. Chem. Eng. J. 195, 103–111.

Li, F.B., Wang, X.G., Zhou, S.G., Liu, C.S., 2006. Reviews on abiotic transformation of organchlorines on the interface of iron oxides and water in red soil colloids. Ecol. Environ. 15, 1341–1351.

Li, J.Y., Xu, R.K., Zhang, H., 2012. Iron oxides serve as natural anti-acidification agents in highly weathered soils. J. Soils Sediments 12 (6), 876–887.

Li, X.C., Yang, Z.Z., Zhang, C., Wei, J.J., Zhang, H.Q., Li, Z.H., Ma, C., Wang, M.M., Chen, J.Q., Hu, J.W., 2019. Effects of different crystalline iron oxides on immobilization and bioavailability of Cd in contaminated sediment. Chem. Eng. J. 373, 307–317.

Lin, J.J., Sun, M.Q., Su, B.L., Owens, G., Chen, Z.L., 2019. Immobilization of cadmium in polluted soils by phytogenic iron oxide nanoparticles. Sci. Total Environ. 659, 491–498.

Liu, R., Altschul, E.B., Hedin, R.S., Nakles, D.V., Dzombak, D.A., 2014. Sequestration enhancement of metals in soils by addition of iron oxides recovered from coal mine drainage sites. Soil Sediment Contam. 23, 374–388.

Liu, R.Q., Zhao, D.Y., 2007. Reducing leachability and bioaccessibility of lead in soils using a new class of stabilized iron phosphate nanoparticles. Water Res. 41, 2491–2502.

Loganathan, P., Vigneswaran, S., Kandasamy, J., Naidu, R., 2012. Cadmium sorption and desorption in soils: a review. Crit. Rev. Environ. Sci. Technol. 42, 489–533.

Mariussen, E., Johnsen, I.V., Strømseng, A.E., 2018. Application of sorbents in different soil types from small arms shooting ranges for immobilization of lead (Pb), copper (Cu), zinc (Zn), and antimony (Sb). J. Soils Sediments 18, 1558–1568.

Min, X.B., Li, Y.W.J., Ke, Y., Shi, M.Q., Chai, L.Y., Xue, Ke, 2017. Fe-FesS$_2$ adsorbent prepared with iron powder and pyrite by facile ball milling and its application for arsenic removal. Water Sci. Technol. 76 (1), 192–200.

Memoli, V., Eymar, E., García–Delgado, C., Esposito, F., Santorufo, L., De Marco, A., Barile, R., Maisto, G., 2018a. Total and fraction content of elements in volcanic soil: natural oranthropogenic derivation. Sci. Total Environ. 625, 16–26.

Memoli, V., Eymar, E., García-Delgado, C., Esposito, F., Panico, S.C., De Marco, A., Barile, R., Maisto, G., 2018b. Soil element fractions affect phytotoxicity, microbial biomass and activity in volcanic areas. Sci. Total Environ. 636, 1099–1108.

Mignardi, S., Corami, A., Ferrini, V., 2012. Evaluation of the effectiveness of phosphate treatment for the remediation of mine waste soils contaminated with Cd, Cu, Pb, and Zn. Chemosphere 86 (4), 354–360.

Ministry of Environmental Protection (MEP) and Ministry of Land and Resources (MLS), P. R. China, 2014. Report on the National Soil Contamination Survey. (in Chinese).

Negassa, W., Leinweber, P., 2009. How does the Hedley sequential phosphorus fractionation reflect impacts of land use and management on soil phosphorus: a review. J. Plant Nutr. Soil Sci. 172, 305–325.

Neidhardt, H., Schoeckle, D., Schleinitz, A., Eiche, E., Berner, Z., Tram, P.T., Chatterjee, D., 2018. Biogeochemical phosphorus cycling in groundwater ecosystems–Insights from South and Southeast Asian flood plain and delta aquifers. Sci. Total Environ. 644, 1357–1370.

Oppong-Anane, A.B., Quiñones, K.Y.D., Harris, W., Townsend, T., Bonzongo, J.C.J., 2018. Iron reductive dissolution in vadose zone soils: implication for groundwater pollution in landfill impacted sites. Appl. Geochem. 94, 21–27.

Qiu, Z.B., Liu, X., Tian, X.J., Yue, M., 2008. Effects of CO$_2$ laser pretreatment on drought stress resistance in wheat. J. Photochem. Photobiol., B 90 (1), 17–25.

Rinklebe, J., Antoniadis, V., Shaheen, S.M., Rosche, O., Altermann, M., 2019. Health risk assessment of potentially toxic elements in soils along the Central Elbe River, Germany. Environ. Int. 126, 76–88.

Shang, E.P., Xu, E.Q., Zhang, H.Q., Huang, C.H., 2018. Spatial-temporal trends and pollution source analysis for heavy metal contamination of cultivated soils in five major grain producing regions of China. Environ. Sci. 39 (10), 4670–4683 (in Chinese).

Sun, R.J., Chen, J.H., Fan, T.T., Zhou, D.M., Wang, Y.J., 2018. Effect of nanoparticle hydroxyapatite on the immobilization of Cu and Zn in polluted soil. Environ. Sci. Pollut. Res. 25 (1), 73–80.

Tiessen, H., Moir, J., 1993. Characterization of available P by sequential extraction. In: Carter, M.R. (Ed.), Soil Sampling and Methods of Analysis. CRC Press Inc, Boca Raton Florida USA, pp. 75–86.

Wang, D.J., Jin, Y., Jaisi, D.P., 2015. Effect of size-selective retention on the cotransport of hydroxyapatite and goethite nanoparticles in saturated porous media. Environ. Sci. Technol. 49 (14), 8461–8470.

Wang, S., Zhao, M., Zhou, M., Zhao, Y., Li, Y.C., Gao, B., Feng, K., Yin, W.Q., Ok, Y.S., Wang, X.Z., 2019. Biomass facilitated phase transformation of natural hematite at high temperatures and sorption of Cd^{2+} and Cu^{2+}. Environ. Int. 124, 473–481.

Wei, L., Wang, S., Zuo, Q., Liang, S., Shen, S., Zhao, C., 2016. Nano-hydroxyapatite alleviates the detrimental effects of heavy metals on plant growth and soil microbes in e-waste-contaminated soil. Environ. Sci-Proc. Imp. 18 (6), 760–767.

Wen, J., Yi, Y., Zeng, G., 2016. Effects of modified zeolite on the removal and stabilization of heavy metals in contaminated lake sediment using BCR sequential extraction. J. Environ. Manag. 178, 63–69.

Wu, B., Amelung, W., Xing, Y., Bol, R., Berns, A.E., 2018. Iron cycling and isotope fractionation in terrestrial ecosystems. Earth Sci. Rev. 190, 323–352.

Xu, C., Yang, W., Zhu, L., Juhasz, A.L., Ma, L.Q., Wang, J., 2017a. Remediation of polluted soil in China: policy and technology bottlenecks. Environ. Sci. Technol. 51, 14027–14029.

Xu, C.Y., Xu, R.K., Li, J.Y., Deng, K.Y., 2017b. Phosphate-induced aggregation kinetics of hematite and goethite nanoparticles. J. Soils Sediments 17 (2), 352–363.

Yin, H., Tan, N.H., Liu, C.P., Wang, J.J., Liang, X.L., Qu, M.K., Feng, X.H., Qiu, G.H., Tan, W.F., Liu, F., 2016. The associations of heavy metals with crystalline iron oxides in the polluted soils around the mining areas in Guangdong Province, China. Chemosphere 161, 181–189.

Yu, H.Y., Li, F.B., Liu, C.S., Huang, W., Liu, T.X., Yu, W.M., 2016. Iron redox cycling coupled to transformation and immobilization of heavy metals: implications for paddy rice safety in the red soil of South China. Advances in Agronomy, vol. 137. Academic Press, pp. 279–317.

Yuan, C., Li, F., Cao, W., Yang, Z., Hu, M., Sun, W., 2019. Cadmium solubility in paddy soil amended with organic matter, sulfate, and iron oxide in alternative watering conditions. J. Hazard Mater. 378, 120672.

Yuan, L., Liu, Y.S., 2013. Removal of Pb(II) and Zn(II) from aqueous solution by ceramisite prepared by sintering bentonite, iron powder and activated carbon. Chem. Eng. J. 215–216, 432–439.

Zhang, C., Yu, Z.G., Zeng, G.M., Jiang, M., Yang, Z.Z., Cui, F., Zhu, M., Shen, L., Hu, L., 2014. Effects of sediment geochemical properties on heavy metal bioavailability. Environ. Int. 73, 270–281.

Zhang, C., Yu, Z., Zeng, G., Huang, B., Dong, H., Huang, J., Yang, Z., Wei, J., Hu, L., Zhang, Q., 2016. Phase transformation of crystalline iron oxides and their adsorption abilities for Pb and Cd. Chem. Eng. J. 284, 247–259.

Zhang, F.Q., Wang, Y.S., Lou, Z.P., Dong, J.D., 2007. Effect of heavy metal stress on antioxidative enzymes and lipid peroxidation in leaves and roots of two mangrove plant seedlings (*Kandelia candel* and *Bruguiera gymnorrhiza*). Chemosphere 67 (1), 44–50.

Zhao, F.J., Ma, Y., Zhu, Y.G., Tang, Z., McGrath, S.P., 2015. Soil contamination in China: current status and mitigation strategies. Environ. Sci. Technol. 49, 750–759.

Zhou, D.M., Jin, S.Y., Wang, Y.J., Wang, P., Weng, N.Y., Wang, Y., 2012. Assessing the impact of iron-based nanoparticles on pH, dissolved organic carbon, and nutrient availability in soils. Soil Sediment Contam. 21 (1), 101–114.

Zhu, M., Hu, X., Tu, C., Zhang, H., Song, F., Luo, Y., Christie, P., 2019. Sorption mechanisms of diphenylarsinic acid on ferrihydrite, goethite and hematite using sequential extraction, FTIR measurement and XAFS spectroscopy. Sci. Total Environ. 669, 991–1000.